ELSEVIER

Computers and Geotechnics 25 (1999) 45–55

COMPUTERS AND GEOTECHNICS

www.elsevier.com/locate/compgeo

Technical Note

Displacement charts for slopes subjected to seismic loads

Liangzhi You [a], Radoslaw L. Michalowski [a,b,*]

[a] *Department of Civil Engineering, The Johns Hopkins University, Baltimore, MD 21218, USA*
[b] *Department of Civil and Environmental Engineering, The University of Michigan, Ann Arbor, MI 48109, USA*

Received 4 January 1999; received in revised form 19 May 1999; accepted 2 June 1999

Abstract

Earthquake events in recent years have brought about renewed interest in analyses of slopes subjected to seismic loads. These loads have been accounted for traditionally by using quasi-static loads. Such analyses do not provide any information about permanent displacements, and they neglect the history of seismic shaking. The analysis presented in this note is based on the rigid block displacement technique. A rotational mechanism of slope failure, caused by horizontal shaking, is considered. Yield accelerations are calculated for uniform slopes, and irreversible displacements are calculated for different earthquake records. The displacements can be represented as the product of a coefficient characteristic of a given collapse mechanism and a double time integral of an earthquake acceleration record. Charts are produced to make the application of the results effortless.

1. Introduction

Geotechnical structures, such as slopes, subjected to earthquake loads are routinely designed using quasi-static design loads. Such an analysis does not give any insight into the behavior of a structure, neglects the seismic process (acceleration history), and does not yield any information about permanent displacements of the structure. A displacement-based design method was suggested more than 30 years ago [1], with a relatively simple one-block translational mechanism. For slopes, however, the most adverse failure pattern known is the one where the soil mass rotates as one rigid body, separated from the stationary soil by a failure surface. An

* Corresponding author. Fax: + 1-734-764-4292.
E-mail address: rlmich@umich.edu (R.L. Michalowski)

0266-352X/99/$ - see front matter
PII: S0266-352X(99)00016-6

extension of the classical sliding rigid block analysis to rotational collapse was suggested in [2]. Calculation results of permanent displacements of slopes will be produced here for different earthquake records.

Although displacement analysis based on a single sliding block consideration was suggested in the nineteen-sixties [1], a renewed interest in this technique was caused by recent earthquake events [3,4]. Some clarifications are offered in this note that relate to the application of the sliding rigid block model to the rotational mechanism.

2. Displacement mechanism

A collapse mechanism of a slope is presented in Fig. 1. During failure the soil mass ABC rotates about center O. Such a mechanism is kinematically admissible from the standpoint of plasticity, and it was considered by Chen et al. [5], and later by Chang et al. [2] in the context of seismic loads. The inclination of the slope is described by angle β, the soil is characterized by its internal friction angle φ and cohesion c, and the geometry of the failure surface is determined by angles θ_0 and θ_h. The toe failure surface shown in Fig. 1(a) is characteristic of frictional soils. Only if the internal friction angle is very small (less than 10°) does the slip surface passing below the toe become more critical for gentle slopes [6]. However, below-the-toe failures become critical for slopes with larger soil internal friction angles if they are subjected to horizontal shaking. For instance, the critical yield accelerations represented by dashed lines in Fig. 2(a,b) are associated with below-the-toe failure surfaces. An additional comment related to these mechanisms is inserted in the last paragraph of this section. For brevity, analytical derivation is shown only for the toe failure surface, but the results in the charts include both the toe and below-the-toe failures, whichever is more adverse.

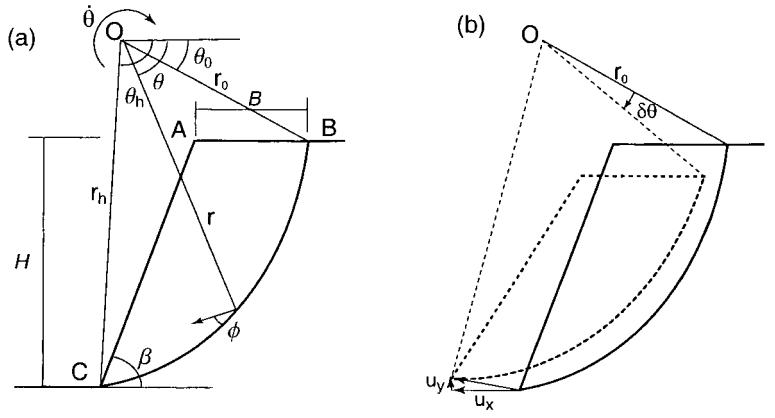

Fig. 1. Rotational collapse of a slope: (a) failure mechanism, and (b) displacement pattern.

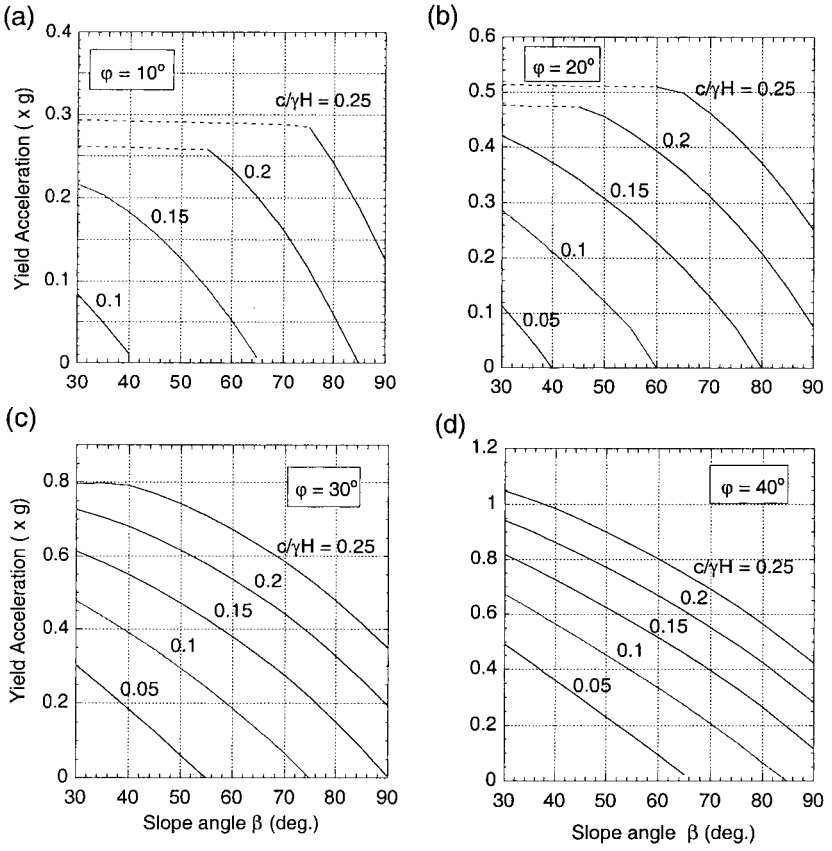

Fig. 2. Critical horizontal acceleration for earth slopes.

Failure surface BC in Fig. 1(a) is a segment of a log-spiral. The moment of the soil weight of block ABC about point O is calculated as the moment of fictitious block BCO about O minus the moments of ABO and ACO about O

$$M_w = \gamma r_0^3 (f_1 - f_2 - f_3) \tag{1}$$

where γ is the unit weight of the soil, r_0 is shown in Fig. 1, and coefficients f_i are functions of β, θ_0, θ_h, and internal friction angle of the soil φ; they can be found in Appendix A. Assuming the entire block ABC is subjected only to horizontal shaking as one rigid body, the moment caused by inertial forces can be calculated analogously as

$$M_s = k\gamma r_0^3 \left(f_1^s - f_2^s - f_3^s\right) \tag{2}$$

where k is the seismic coefficient representing horizontal acceleration as a fraction of the gravity acceleration (see Appendix A for coefficients f_i^s). The two moments, M_w and M_s, are counterbalanced by the moment of the shear resistance of the soil along surface BC

$$M_c = \frac{cr_0^2}{2\tan\varphi}\left(e^{2(\theta_h-\theta_0)\tan\varphi} - 1\right) \tag{3}$$

where c is the soil cohesion, and φ is the angle of internal friction of the soil.

At the verge of failure the horizontal acceleration reaches the level of yield acceleration (or critical acceleration), $k_c g$ (g being the gravity acceleration), and the equation of moment equilibrium becomes

$$\gamma r_0^3\left[(f_1 - f_2 - f_3) + k_c\left(f_1^s - f_2^s - f_3^s\right)\right] = \frac{cr_0^2}{2\tan\varphi}\left(e^{2(\theta_h-\theta_0)\tan\varphi} - 1\right) \tag{4}$$

However, when the rotational acceleration of block ABC about O is not zero ($\ddot{\theta} \neq 0$, and $k \neq k_c$), an additional moment, due to inertial forces, will appear in the equation of motion

$$\gamma r_0^3\left[(f_1 - f_2 - f_3) + k\left(f_1^s - f_2^s - f_3^s\right)\right] = \frac{cr_0^2}{2\tan\varphi}\left(e^{2(\theta_h-\theta_0)\tan\varphi} - 1\right) + \frac{G}{g} l^2\ddot{\theta} \tag{5}$$

where $\ddot{\theta}$ is the rotational acceleration of the block about point O, G is the weight of the rotating block, and l is the distance from point O to the center of gravity of block ABC (expressions for both G and l can be found in Appendix A). Subtracting Eq. (4) from Eq. (5) and rearranging, one obtains

$$\ddot{\theta} = (k - k_c)\frac{\gamma r_0^3}{\frac{G}{g} l^2}\left(f_1^s - f_2^s - f_3^s\right) \tag{6}$$

Expressions similar to Eq. (6), for both translational and rotational mechanisms, were developed by Chang et al. [2]. The motion of the block starts when the seismic acceleration first exceeds the yield (critical) acceleration, and the velocity of the block increases for as long as the ground acceleration exceeds the critical acceleration of the structure. The velocity of the block reaches its maximum when the seismic acceleration drops down again to the critical level for the structure. The relative movement of the block and the soil it slides on ceases in the relative deceleration process, which happens when the seismic acceleration drops to some value below the critical level. The permanent rotation increment $\delta\theta$ can now be found by double integrating block acceleration $\ddot{\theta}$ over time interval δt

$$\delta\theta = \int_{\delta t}\int_{\delta t} \ddot{\theta}\,\mathrm{d}t\,\mathrm{d}t \tag{7}$$

The maximum horizontal displacement, δu_x, of the slope face occurs at the toe, and its increment can be calculated as [angle $\delta\theta$ not exceeding 15°, or $\delta\theta \approx \tan(\delta\theta)$]

$$\delta u_x = r_h \delta\theta \sin\theta_h = \frac{\gamma r_0^4}{Gl^2} e^{(\theta_h-\theta_0)\tan\varphi}\left(f_1^s - f_2^s - f_3^s\right)\int_{\delta t}\int_{\delta t} g(k-k_c)\mathrm{d}t\mathrm{d}t$$
$$= C\int_{\delta t}\int_{\delta t} g(k-k_c)\mathrm{d}t\mathrm{d}t \tag{8}$$

The expression in the front of the integral in Eq. (8) is denoted here by C, and it appears to be a dimensionless coefficient (see Appendix A for G and l, and note that G is in units of weight per unit length in the direction perpendicular to the plane of deformation). Coefficient C relates the displacement of the slope toe to the integral of the acceleration record above the level of the yield acceleration. This coefficient is characteristic of the displacement mechanism chosen, and its particular form here was derived for the rotational mechanism which has the most adverse pattern of all known admissible collapse modes for slopes. While coefficient C is characteristic of the slope and soil properties, the double integral in Eq. (8) can be calculated without reference to a specific structure, other than its yield acceleration coefficient k_c. This integral can be calculated for a given earthquake record for a range of hypothetical yield accelerations, and is used later for estimation of permanent displacements of any structure for which coefficient C and the yield acceleration are known.

The expression in Eq. (4) was used to calculate the critical (yield) acceleration of slopes. For a slope of given inclination (β) and for a given internal friction of the soil (φ). The results of calculations are shown in Fig. 2. The yield acceleration coefficient, k_c, for uniform slopes can be found from the expression in Eq. (4) as

$$k_c = \frac{1}{2\tan\varphi}\,\frac{H}{r_0}\,\frac{e^{2(\theta_h-\theta_0)\tan\varphi}-1}{f_1^s - f_2^s - f_3^s}\,\frac{c}{\gamma H} - \frac{f_1 - f_2 - f_3}{f_1^s - f_2^s - f_3^s} \tag{9}$$

where the slope is characterized by dimensionless parameter $\gamma H/c$ (γ is the unit weight of soil, c is the cohesion, and H is the slope height), slope inclination angle β, and internal friction angle of the soil φ [see in Appendix A for H/r_0]. The minimum of k_c was sought from Eq. (9) with angles θ_0 and θ_h being variable. Although values of k_c for simple slopes can be found elsewhere [2], they were recalculated here for a wider range of parameters, and they are given in Fig. 2.

When $\varphi \approx 0$ the critical collapse mechanism includes a failure surface which passes below the toe, and the overall size of the most critical mechanism increases to orders of magnitude larger than the slope height. For a large failure mass (where the slope height becomes insignificant with respect to the overall size of the deep-seated mechanism), and when $\varphi \approx 0$, the solution becomes independent of the soil weight. The stabilizing effect of the shear resistance along the failure surface increases linearly with the mechanism size, whereas the adverse effect caused by the horizontal shaking increases with the square of the size. Hence, the increase in the size of the failure mass, when $\varphi \approx 0$, is not surprising. This effect is seen also for larger internal friction angles, and the solutions indicated by dashed lines in Fig. 2(a) and (b) relate

to this effect. It should be noticed, however, that the solutions for a large failure mass are not realistic since the assumption that all of the soil mass (orders of magnitude larger than the slope height) is in the same shaking phase is not reasonable. This effect is different from the out-of-phase response of high slopes subjected to base excitations. The former is a computational effect related to the assumption of uniform acceleration field, whereas the latter is a true effect associated with propagation of the base shaking through the soil above.

3. Displacement charts

Coefficient C was calculated for a wide range of slopes, and is presented in Fig. 3 for different β, φ, and yield acceleration k_c. Angles θ_0 and θ_h that describe the log-spiral surface (Fig. 1) were not given a priori, but they were calculated such that k_c in Eq. (9) was a minimum for given $\gamma H/c$, β, and φ. Hence, coefficient C can be

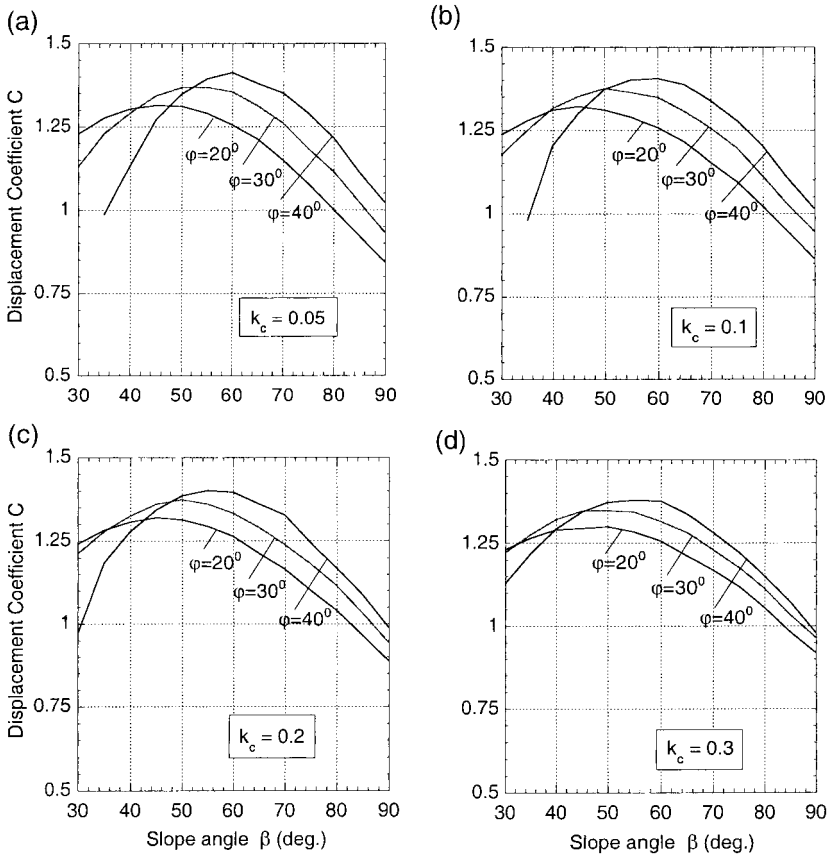

Fig. 3. Displacement coefficient for rotational collapse of slopes subjected to seismic loads.

represented as a function of only three parameters, for instance, $\gamma H/c$, β, and φ. It is convenient, however, to show C as a function of k_c, β, and φ, since k_c appears explicitly in the double integral in Eq. (8) (i.e. out of parameters $\gamma H/c$, β, φ, and k_c, only three are independent).

The double integral in Eq. (8) was calculated for four different earthquake records: El Centro 1940, San Fernando 1971, Big Bear Lake 1992, and Northridge 1994. The details of these earthquake records are given in Table 1. The Northridge (Moorpark Station) record of horizontal ground acceleration is shown in Fig. 4(a). A time integral of this record above the threshold of $k_c = 0.05$ is presented in Fig. 4(b), and a double time integral is shown in Fig. 4(c). These integrals can be interpreted as the velocity and the displacement of a fictitious block on a horizontal, but anisotropic, surface (with critical acceleration dependent on the orientation, and being exceeded only in one direction). The threshold acceleration is the yield acceleration of the block (structure). This is a typical scheme of finding permanent displacements in translation mechanisms. The double time integral appears in Eq. (8) for a realistic rotational slope failure mechanism, thus, one can find the displacement for such a mechanism by multiplying this integral [Fig. 4(c)] by an appropriate coefficient C (Fig. 3).

To make the results easily applicable in practice, the double integral in Eq. (8) was calculated for different earthquake acceleration records. The peak acceleration (k_m) in each record was scaled to a series of accelerations in such a way so that the integral in Eq. (8) could be represented as a function of the difference between the peak acceleration of the ground and the yield acceleration of the structure ($k_m - k_c$), for different yield accelerations of the slopes (k_c). These charts are presented in Fig. 5 for different earthquake records. An illustrative example is presented in the next section.

4. Example

An estimation of an expected permanent displacement of a slope using charts in Figs. 3 and 5 is straightforward. Let the slope have an inclination angle $\beta = 55°$,

Table 1
Earthquake sites

Earthquake	Northridge	Big Bear	San Fernando	Imperial Valley
Date	1/17/94	6/28/92	2/9/71	5/18/40
Recording site	Moorpark	Big Bear Lake	Pacoima Dam	El Centro
CSMIP[a] station	No. 24283	No. 22561	No. 279	No. 117
Magnitude	6.7	6.6	6.4	6.7
Direction	180°	270°	S74W	S00E
Peak accel. (cm/s^2)	286.18	472.17	1054.94	341.69
Epicenter distance	23 km	13 km	7 km	9 km

[a] California strong motion instrumentation program.

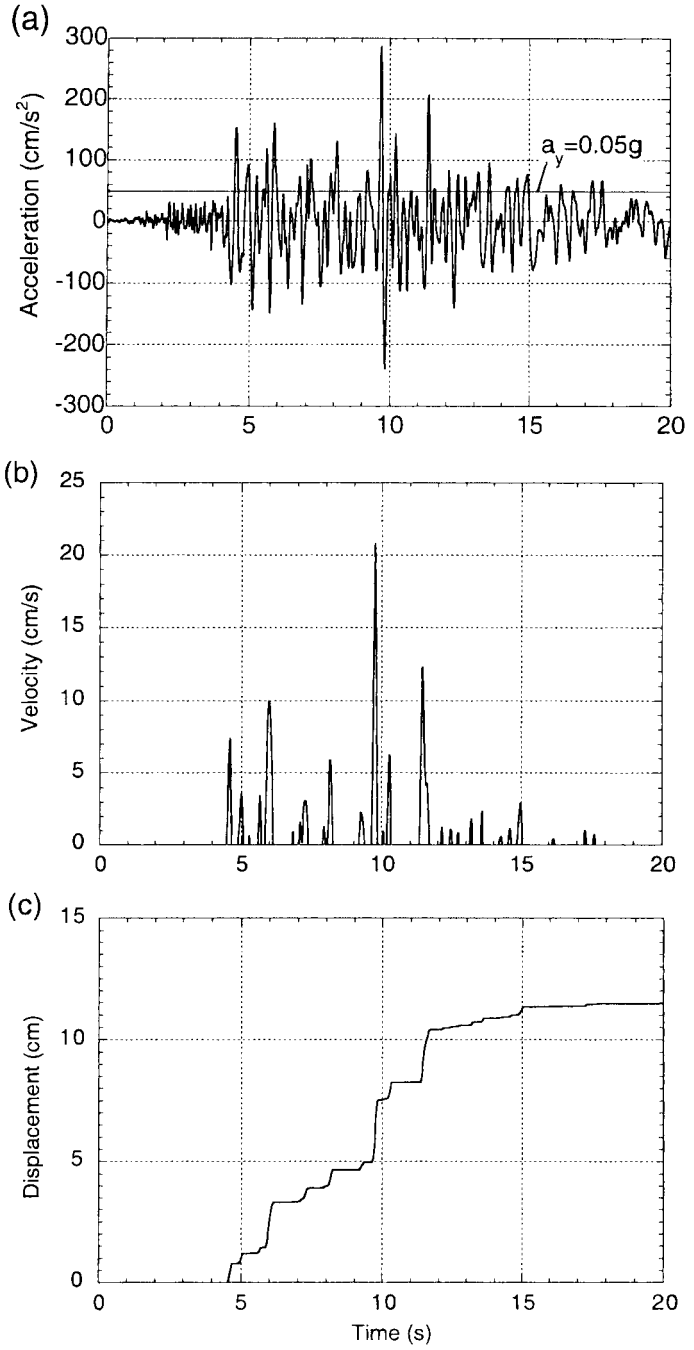

Fig. 4. Northridge 1994 earthquake record (Moorpark Station): (a) horizontal ground acceleration, (b) velocity of a block on a horizontal (but anisotropic) surface, and (c) block displacement with respect to the ground surface.

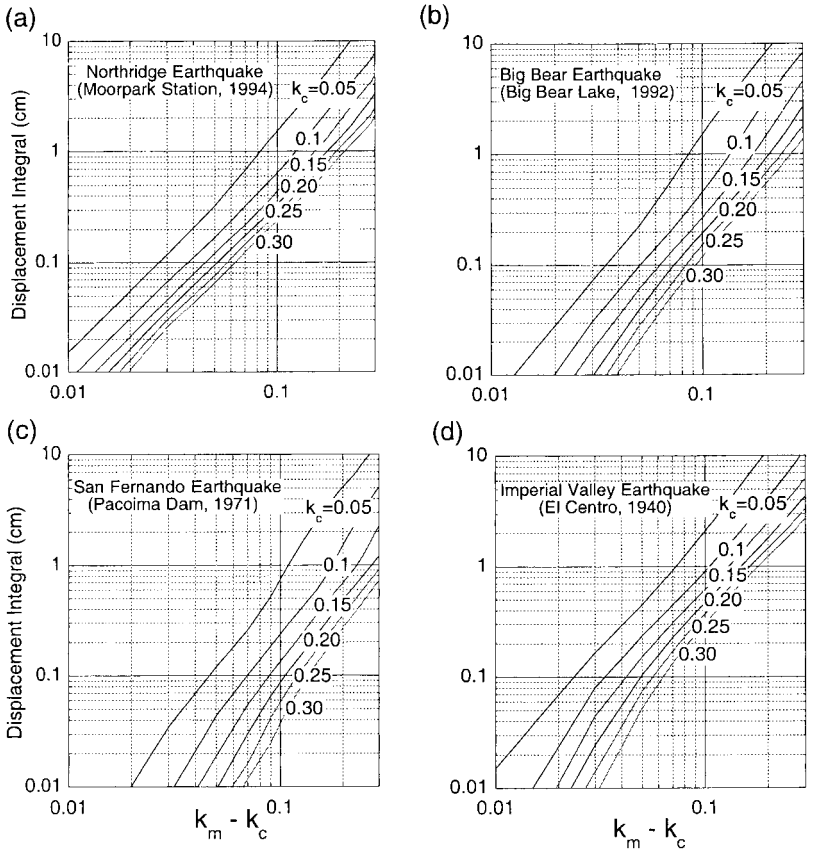

Fig. 5. Displacement integrals of horizontal acceleration records: (a) Northridge 1994, (b) Big Bear Earthquake 1992, (c) San Fernando 1971, and (d) El Centro 1940.

height $H=18$ m, unit weight of soil $\gamma=17$ kN/m^3, internal friction angle $\varphi=36°$, and cohesion $c=15.3$ kN/m^2 ($c/\gamma H=0.05$). This slope is stable, but it will be at the verge of failure if the horizontal seismic acceleration coefficient reaches its critical value $k_c=0.1$ [this number was interpolated from results in Figs. 2(c) and (d)]. Coefficient C was interpolated from Fig. 3(b) as $C=1.384$ ($C=1.36$ for $\varphi=30°$, and $C=1.40$ for $\varphi=40°$).

Once k_c and C are known, one needs to decide on an earthquake record (expected seismic event). Different records represent different patterns and duration of shaking. The magnitude of the peak acceleration can be selected by choosing an appropriate difference k_m-k_c. For instance, assuming the Northridge record with peak acceleration coefficient $k_m=0.3$, $k_m-k_c=0.2$, and from Fig. 5(a) the displacement integral appears to be equal to 3 cm. Now the expected displacement of the slope toe, according to Eq. (8), is equal to $C\times 3\approx 4.2$ cm.

5. Final remarks

The charts presented make the calculations of permanent displacements of slopes rather simple. Estimating displacement includes three steps: identifying the critical acceleration for a given slope, calculating the coefficient that characterizes the mechanism of slope yielding, and integrating the earthquake record. The product of the coefficient and the time double integral of the earthquake acceleration record (above the critical threshold) gives the horizontal displacement of the toe of the slope. The three steps are reduced here to reading (interpolating) the specific numbers from the charts.

Acknowledgement

The work presented in this paper was sponsored by the National Science Foundation, grants Nos. CMS-9634193 and CMS-9820832. This support is greatly appreciated.

Appendix A: expressions for coefficients f_1–f_3 and $f^{\S}_1$–$f^{\S}_3$

Functions f_1–f_3 were given first by Chen et al. [5] in the context of slope stability analysis, and they are given here for the case of a horizontal crest of the slope (as in Fig. 1)

$$f_1 = \frac{1}{3\left(1+9\tan^2\varphi\right)}\left[\left(3\tan\varphi\cos\theta_h+\sin\theta_h\right)e^{3(\theta_h-\theta_0)\tan\varphi}-3\tan\varphi\cos\theta_0-\sin\theta_0\right] \tag{10}$$

$$f_2 = \frac{1}{6}\,\frac{B}{r_0}\left(2\cos\theta_0-\frac{B}{r_0}\right)\sin\theta_0 \tag{11}$$

$$f_3 = \frac{1}{6}\,\frac{H}{r_0}\,\frac{\sin(\beta+\theta_h)}{\sin\beta}\left(2\cos\theta_h e^{(\theta_h-\theta_0)\tan\varphi}+\frac{H}{r_0}\cot\beta\right)e^{(\theta_h-\theta_0)\tan\varphi} \tag{12}$$

where

$$\frac{B}{r_0} = \frac{1}{\sin\theta_h}\left[\sin(\theta_h-\theta_0)-\frac{H}{r_0}\,\frac{\sin(\beta+\theta_h)}{\sin\beta}\right] \tag{13}$$

and

$$\frac{H}{r_0} = \sin\theta_h e^{(\theta_h-\theta_0)\tan\varphi}-\sin\theta_0 \tag{14}$$

Expressions for f_1^s–f_3^s were used by Chang et al. [2], and they were rederived here

$$f_1^s = \frac{1}{3\left(1+9\tan^2\varphi\right)}\left[(3\tan\varphi\sin\theta_h - \cos\theta_h)\mathrm{e}^{3(\theta_h-\theta_0)\tan\varphi} - 3\tan\varphi\sin\theta_0 + \cos\theta_0\right] \tag{15}$$

$$f_2^s = \frac{1}{3}\,\frac{B}{r_0}\sin^2\theta_0 \tag{16}$$

$$f_3^s = \frac{1}{6}\,\frac{H}{r_0}\,\frac{\sin(\beta+\theta_h)}{\sin\beta}\left(2\sin\theta_h\mathrm{e}^{(\theta_h-\theta_0)\tan\varphi} - \frac{H}{r_0}\right)\mathrm{e}^{(\theta_h-\theta_0)\tan\varphi} \tag{17}$$

Expressions for the weight G of block ABC (Fig. 1) and the distance l from the center of gravity to the center of rotation are

$$G = \frac{1}{2}\gamma r_0^2\left[\frac{\mathrm{e}^{2(\theta_h-\theta_0)\tan\varphi}-1}{2\tan\varphi} - \frac{B}{r_0}\sin\theta_0 - \frac{H}{r_0}\,\frac{\mathrm{e}^{(\theta_h-\theta_0)\tan\varphi}\sin(\beta+\theta_h)}{\sin\beta}\right] \tag{18}$$

and

$$l = \frac{\gamma r_0^3}{G}\sqrt{(f_1-f_2-f_3)^2+\left(f_1^s-f_2^s-f_3^s\right)^2} \tag{19}$$

References

[1] Newmark NM. Effects of earthquakes on dams and embankments. Géotechnique 1965;15:139–60.

[2] Chang C-J, Chen WF, Yao JP. Seismic displacements in slopes by limit analysis. J Geot Engrg 1984;110(7):860–74.

[3] Ling HI, Leshchinsky D. Seismic performance of simple slopes. Soils and Foundations 1995;35(2):85–94.

[4] Cai Z, Bathurst RJ. Deterministic sliding block methods for estimating seismic displacements of earth structures. Soil Dynamics and Earthquake Engineering 1996;15:255–68.

[5] Chen WF, Giger MW, Fang HY. On the limit analysis of stability of slopes. Soils and Foundations 1969;9(4):23–32.

[6] Chen WF, Giger MW. Limit analysis of stability of slopes. J Soil Mech Found Engrg 1971;97(1):19–26.